Compact and efficient RGB to RGBW data conversion method and its application in OLED microdisplays

Chi Can (SID Student Member)
Ian Underwood (SID Member)

***Abstract* —** In many electronic information displays, a colour pixel comprises three spatially distinct sub-pixels containing red, green and blue (RGB) colour filters. The option of adding a fourth white (W) sub-pixel that allows light to pass through unfiltered can significantly improve the optical efficiency of the pixel that, in turn, increases the power efficiency of the display. Such a display is called an RGBW display, and the required transformation of data format from incoming RGB to pixel RGBW is termed as "RGB to RGBW conversion." This paper reports a method of RGB to RGBW conversion that is highly compact and efficient in terms of system resources while retaining image quality. It processes incoming data through a new colour space conversion algorithm in order to reduce the average power consumption with no noticeable visual artefacts. We explain the method and demonstrate its cost-effective and power-effective implementation for the specific case of an organic light emitting diode microdisplay.

Keywords *— organic light emitting diode (OLED), microdisplay, RGBW, RGB-to-RGBW.*
DOI # 10.1002/jsid.158

1 Introduction

Colour is achieved in most electronic information displays (EIDs) through the pixel configuration of a triad comprising three spatially separate red, green and blue (RGB) sub-pixels. When a white backlight is projected through RGB colour filters (CFs), the overall optical efficiency of the system is low. Recent reports[1–3] describe the improvements that can be achieved by the addition of a white sub-pixel (WSP) to create a quad RGBW pixel. In a quad-sub-pixel architecture, three of the sub-pixels are covered by the RGB CFs as before, and the WSP is covered by a transparent filter or no filter, thus allowing unfiltered transmission of the white illumination. This unfiltered transmission through the WSP reduces the overall light loss due to absorption by the CFs and so has the potential to increase the luminance output of a display with RGBW pixels for a given power consumption or decrease the power consumption required to achieve a given luminance.

The WSP brings different benefits to different display technologies using CFs to generate colours[4,5] (Fig. 1). For a non-self-illuminated display, such as a liquid crystal display (LCD) with a backlight of constant intensity, the WSP is more beneficial for the display system in terms of white *enhancement* (Fig. 1d), which uses the WSP to increase the overall transmissivity of the backlight through the display system. For a self-illuminated display, such as organic light emitting diode (OLED) with white emission and RGB CFs, the WSP is more beneficial for the display system in terms of white *replacement* (Fig. 1e), which uses the WSP to replace partial backlight transmission from colour sub-pixels covered by CFs.

An OLED display has an organic light-emitting stack on top of the active-matrix substrate. Within each pixel, the OLED (Fig. 2) luminance is controlled by an applied current[6] or voltage.[7] The relative merits of current drive and voltage drive are well known.[8,9]

In the case of microdisplays, an OLED display optical architecture (Fig. 3) has distinct advantages over other technologies such as liquid crystal on silicon (LCoS) and digital micro-mirror device (DMD), especially in terms of the simple optical arrangement and for the relatively low power consumption particularly when displaying predominantly low-brightness content (such as movies and television programmes). In general, LCoS and DMD display systems generate a constant backlight without regard to the picture content. Also, a certain amount of the light is lost in the polarizing optics of LCoS and in the off image path light deflection of DMD, respectively. In contrast, OLED only emits light when and where it is required. Therefore, there is no energy waste in the dark state in the case of OLED. This makes OLED microdisplay very energy efficient and therefore very suitable for use in battery-powered situations such as a personal near-to-eye application.

For white OLED (WOLED) emission with CF array showing full white content, however, OLED can consume more power than LCD.[10] With an expectation of deploying the OLED microdisplay in battery-powered personal applications[11] and with display-system-on-chip (DSoC) approach,[12] the OLED

Received 09/20/12; accepted 04/09/13.
The authors are with Institute for Integrated Systems, School of Engineering, University of Edinburgh, Edinburgh, UK; e-mail: can.hkg@gmail.com.

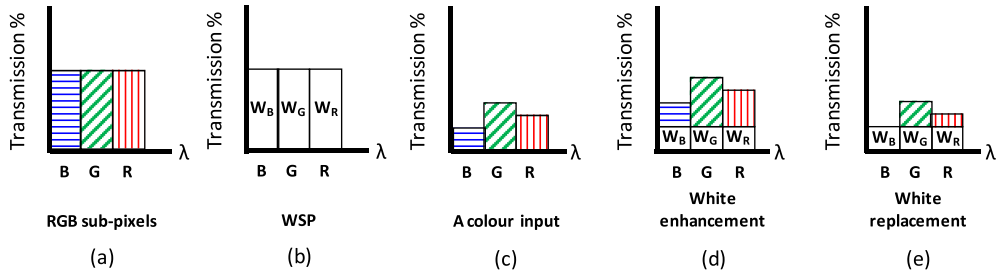

FIGURE 1 — Roles of white sub-pixel (WSP) in white enhancement and white replacement.

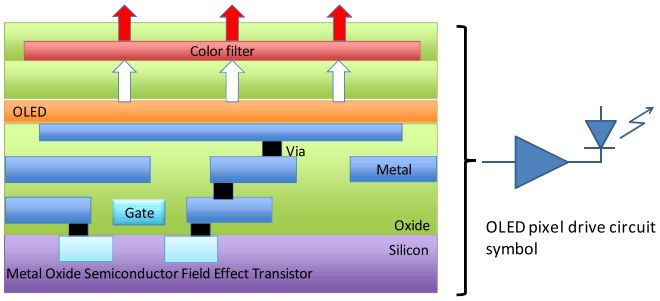

FIGURE 2 — Schematic of a single pixel of organic light emitting diode (OLED).

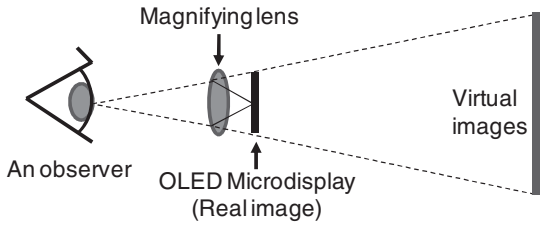

FIGURE 3 — Near-to-eye optics of organic light emitting diode (OLED) display.

microdisplay has to minimize power consumption when displaying the bright image contents in order to preserve the battery useful time.

A colour OLED display using efficient single colour emitters can eliminate the energy reduction from CFs, but this approach is not currently available at the small dimensions required for a microdisplay.[13] A continuous WOLED layer across the sub-pixels facilitates ease of fabrication of the OLED stack at microdisplay dimensions when compared with the patterned colour sub-pixel with colour OLEDs.[14,15] Therefore, the RGBW quad-pixel can offer specific benefits to the OLED *microdisplay*. The WSP is able to increase the useful lifetime of the OLED pixels by lowering the individual sub-pixel luminance and required the current through the OLED stack thereby reducing the rate of ageing of the OLED device.[16,17] In other words, the RGBW quad-pixel is able to improve the overall brightness and the lifetime of the display by using the WSP to efficiently replace the white component in the colour inputs.

In addition, the active-matrix backplane of the OLED microdisplay is usually fabricated on crystalline silicon with complementary metal oxide semiconductor (CMOS) process as an active matrix display. A CMOS backplane is able to substantially reduce the number of external electrical connections to the display and is subject to lower manufacturing variation than the thin film transistor technology used in larger conventional LCDs. As a result, CMOS provides an emissive OLED microdisplay with a high potential to achieve DSoC[13]—that is a display technology with a high level of overall system integration. This approach has the worthwhile aim to integrate on the CMOS active matrix backplane all of the electrical and electro-optical components that are necessary to form the complete display system.

In a low cost, low power DSoC-based RGBW OLED microdisplay, a compact and efficient RGB-to-RGBW conversion (CE-RRC) method is necessary to generate the data value for the WSP from the incoming RGB data. The CE-RRC must be capable of integration on the CMOS crystalline silicon backplane. In a chip level design, the complexity of an algorithm highly affects the footprint and system power consumption.[18] Therefore, our CE-RRC should minimize the use of memory and the number of arithmetic operations in order to achieve the necessary data conversion utilizing the minimum system resource, in other words, very low power consumption. Our strong focus on minimizing the footprint and power consumption of the CE-RRC in order to allow it to be integrated on the CMOS active matrix backplane of the OLED microdisplay with minimal effect on both the cost and the power consumption of the system differentiates this work from previous approaches to CE-RRC.

2 Review of RGB-to-RGBW data conversion methods

Red, green and blue are one of the most basic and widely used colour signal formats for digital EIDs.[19] Starting with RGB format, one additional white (W) signal has to be derived for the WSP in the RGBW system. Therefore, this 3-to-4 data conversion is called RGB-to-RGBW conversion (RRC). The aim of the RRC is to either increase the luminance output or reduce the power consumption of the RGBW display or some combination of both.

The extra luminance from the OLED with RGBW system is derived from the WSP. However, the data conversion to

generate the data value for the WSP is a process that directly changes the optical performance of the RGBW system. For this reason, the particular chromatic properties of the specific flat panel EID must be taken into account in devising the data conversion. To begin with chromatic considerations, there are two generic colour issues that are widely recognized as necessary for proper implementation of a WSP in an RGBW flat panel EID. They are as follows:

(1) the inaccurate assumption that the spectral composition of the white light created by combining the RGB components transmitted through the three CFs, called the reference white (W_{REF}), is the same as the spectral composition of the unfiltered white emitted directly from the WSP (W_{WSP}) and

(2) the incorrect use of subtraction of achromatic component direct from the RGB data inputs.

The first issue concerns the spectral mismatch between the unfiltered white emission and the filtered transmission through the CFs. This can be minimized by a precise colour calibration during the manufacturing.

The second issue, however, is specific for the RRCs[20,21] looking at the white (achromatic) information in a colour input as a constant and using subtraction to remove this achromatic from the colour input directly.

The basis of subtraction of a white constant in the subtractive colour mixing theory relies upon the assumption of a constant white reflection. In an additive colour system such as LCD (or WOLED using CFs), this is not the case. In these systems, the proportion of white at different drive levels is composed by RGB. Unless the RGB intensities are normalized to a corresponding WSP drive level,[22] direct subtraction of achromatic information in the data processing will cause inaccurate optical results as illustrated in Fig. 4.

3 Principles of compact and efficient RGB-to-RGBW conversion

The principle of good RRC design is to study carefully any colour changes caused by the WSP and to design the data conversion to preserve the optical characteristics of the RGWB system to mirror as closely as possible those of the RGB system.

The purpose of the inclusion of the WSP, as previously stated, is to increase the overall brightness and/or to decrease the drive level of RGB sub-pixels displaying bright graphical content. Generic colour issues further raise the point of colour differences between the RGB mode and the RGBW mode in the quad pixel system. The differences can be characterized by using a colour tolerance circle (Fig. 5) that contains a target point defined as a centre for comparison purposes. Any displacement from this centre represents a colour variation.

In Fig. 5, the colour difference obtained by adding the WSP can be calculated by applying Eq. (1) and is expressed as follows:

$$\Delta u'_T v'_T = \sqrt{(u'_{RGB} - u'_{RGBW}) + (v'_{RGB} - v'_{RGBW})} \qquad (1)$$

If C_{RGBW} stays within the colour tolerance circle, it means that C_{RGBW} "looks the same" as C_{RGB}. In terms of signal processing, the ratio of colour outputs (R″ + W″):(G″ + W″):(B″ + W″) should be close to that of the colour inputs R′:G′:B′ with the result that C_{RGBW} is visually indistinguishable from C_{RGB}.

Our suggested RRC uses a simple subtractive approach to calculate the maximum involvement of the WSP, and then use the WSP% to lower the C_{Error} from the WSP into the colour output. To increase the accuracy of the CE-RRC, there is a procedure to calculate the WSP% based on the individual colour region to adjust the reduction of the involvement of the WSP. This is achieved by a semi-colour space conversion. The new CE-RRC is as follows:

$$\begin{aligned} W'' &= MIN[R'G'B'] \times WSP\% \\ R'' &= R' - W\} \\ G'' &= G' - W'' \\ B'' &= B' - W'' \end{aligned} \qquad (2)$$

where

W″ is the output of the WSP,
R″G″B″ are the colour outputs,
R′G′B′ are the colour inputs,
MIN[R′G′B′] is the minimum value of R′,G′ and B′, and
WSP% is the weighting factor of the WSP with regard to the colour inputs.

A core element in the CE-RRC is the "colour group identification" that converts the RGB colour space to a newly introduced pseudo colour space defined by the colour intensive level (CIL). In this colour space, RGB inputs are only referred to different CILs. Therefore, only 1/3 of the data remains after the conversion. The outcome of the "colour group identification"

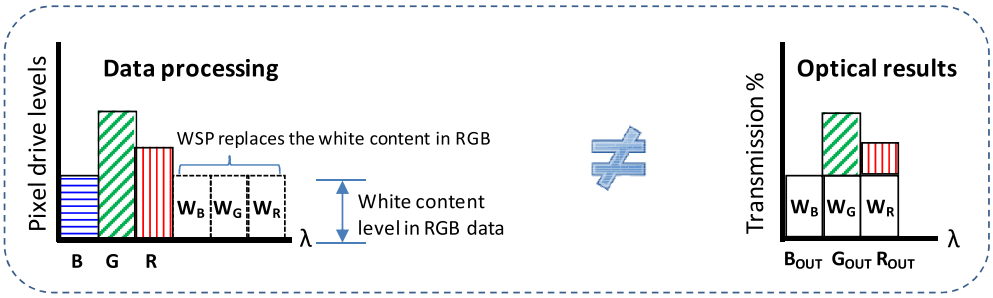

FIGURE 4 — White content replacement using subtractive method.

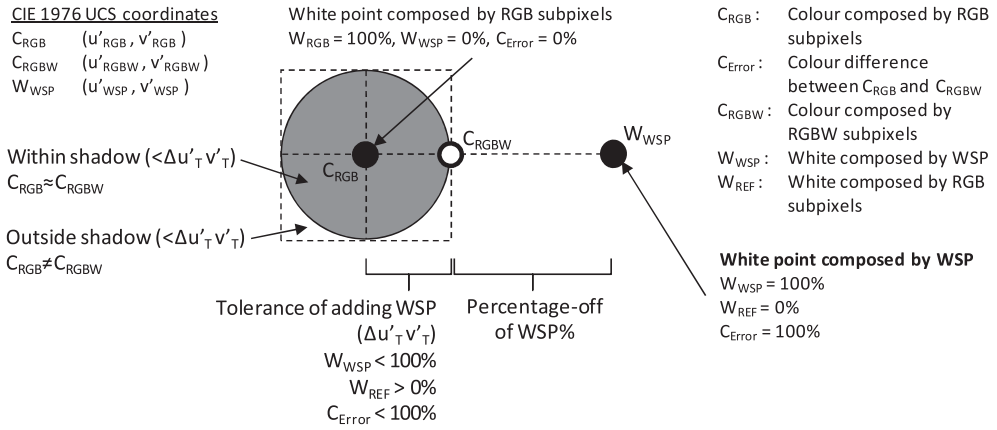

FIGURE 5 — Colour tolerance circle model.

is a CIL combination that classifies a specific ratio of R:G:B in order to assign an appropriate value with which to determine the outputs of the four channels in the RGBW system.

3.1 A pseudo colour space conversion

Figure 6 illustrates a CIL system that represents different colour intensity ratios of R:G:B by combinations of low (L), medium (M) and high (H) intensity values of each. The idea of the conversion from RGB to CIL is based upon the additive colour reproduction (ACR) system. In this system, colours are classified into different hues: primary colour, RGB, and secondary colour, cyan, magenta and yellow (CMY). A colour with approximately equal levels of R, G and B inputs is defined as a neutral colour—white (W). As a result, referring each drive level of a given RGB input as a combination of CILs to set the different ratios of R:G:B into an appropriate colour region.

By neglecting the order of CILs and allowing the repetition of some CILs, some of the combinations are eliminated. For example, LHL and HLL are in the same CIL group as LLH. Hence, the final classification of the CIL regions is obtained as shown in the tabulated list in the lower part of Fig. 6. This way, the three colour data inputs become the CIL combination that is classified into one of the four different colour groups: primary (1°), secondary (2°), neutral (N) and transition (T). In Fig. 6, the primary, secondary and neutral groups are represented by areas; the location of the transition group is approximated by the region on and around the dashed line between the primary and secondary colour groups.

3.2 Three-dimensional colour intensity mapping

After converting the RGB inputs to CIL inputs in the ranges L, M and H, six colour sectors (RGBCMY) of the ACR, as well as the CIL combinations, can be plotted on the CIE (Commission internationale de l'éclairage) chromaticity diagram illustrated as Fig. 7(a) that shows how the six colour sectors are located in the CIE colour map. Then, Fig. 7b is an enlarged partial view (of the area bounded by W, R and M) to show different CIL combinations located in the ACR colour sector.

Each CIL combination is defined by the combination of drive levels of the RGB inputs that form any colour of N, 1°, 2° and T by different ratios of R:G:B. Therefore, the

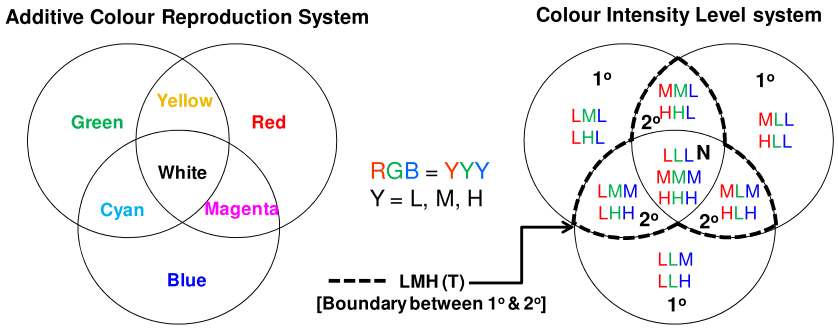

After elimination of repeated combinations (Neglect order and allow repetition):	
Primary (1°) colour group: LLM, LLH	**Neutral (N) colour group:** LLL, MMM, HHH
Secondary (2°) colour group: LMM, LHH	**Transition (T) colour group:** LMH

FIGURE 6 — Conversion of additive colour reproduction system to CIL system.

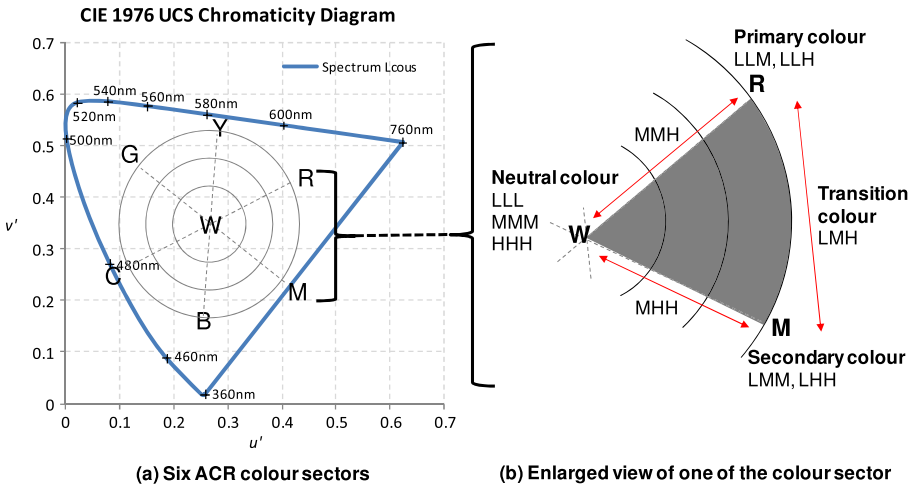

FIGURE 7 — Illustrations of (a) additive colour reproduction (ACR) colour section and (b) enlarged view of one sector.

ratio of L:M:H is the same as the ratio of R:G:B. Different RGB inputs give different combinations of the LMH in different colour sectors, but in terms of intensity, each colour sector is the same. Every sector consists of neutral colours (LLL, MMM, HHH), primary colours (LLM, LLH, MMH), secondary colours (LMM, LHH, MHH) and transition colours (LMH). Therefore, the CE-RRC is required to process only one colour sector instead of six colour sectors (RGBCMY), and this can reduce the volume of data being processed in the later WSP% calculation, which work load of computation bases on the number of colour regions.

The colour sector is on the horizontal plane of the CIE chromaticity diagram, which is two-dimensional (2D). After the transformation of RGB inputs to CIL combinations, the 2D CIL combination map is further transformed into a three-dimensional (3D) pseudo colour space. With regard to the methods suggested by T. Ito[23] and S.D. Lee *et al.*,[24] the 2D colour map is converted into a 3D colour model by defining each

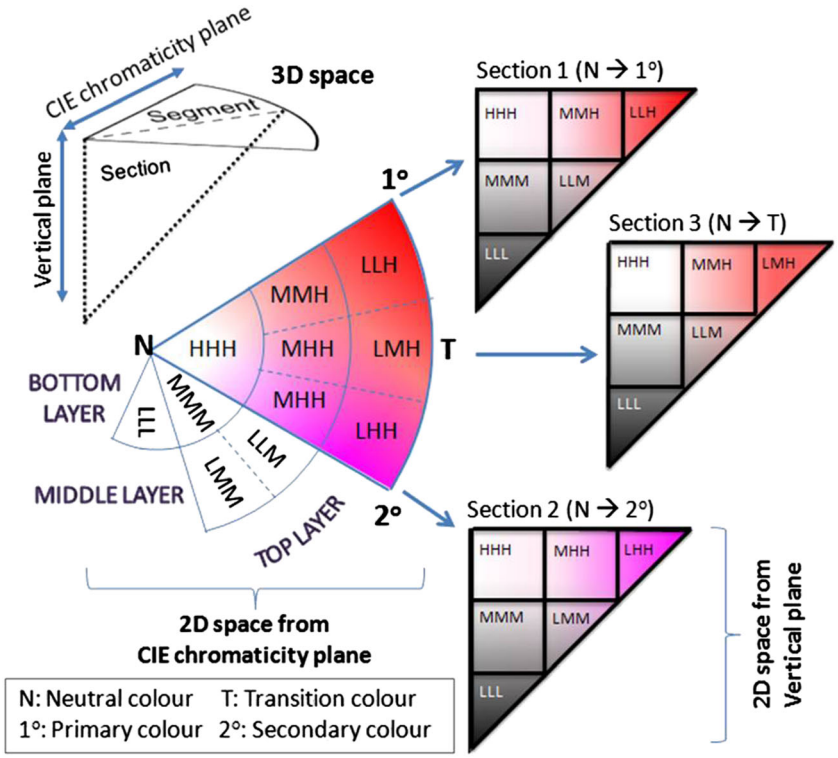

FIGURE 8 — Colour intensive level 3D model.

colour region according to its combination of colours. In the case of the CE-RRC, the third dimension is also determined by the CIL. The CIL 3D model of the colour sector against each colour section is illustrated in Fig. 8.

Initially, the RGB inputs are processed according to their CIL. Each CIL combination is considered as an individual colour region that represents white component information regarding a specific ratio of R:G:B. Thereafter, different coefficients (WSP%) are assigned according to the different colour regions. The initial value of WSP% in each region can be simply looked upon as the ratio of the luminance generated by the RGB sub-pixels (Y_{RGB}) to the luminance generated by the WSP (Y_{WSP}) as shown in Eq. (3). Any further adjustment of WSP% with regard to different colour regions can be carried out if necessary.

$$\mathrm{WSP}\% = \frac{Y_{RGB}}{Y_{WSP}} \times 100\% \tag{3}$$

In short, the RGB inputs are converted into the CIL combinations resulting in a data volume reduction of 2/3. Clearly, this is significant for implementing the RRC in a DSoC configuration in which small area and low power consumption are key drivers.

The CE-RRC avoids resource-intensive colour space conversion (such as from RGB to XYZ, YUV or others as is common in existing RRCs[24,26–28]), thus it can be considered a low power design.[29] Furthermore, a chip area estimate for the CE-RRC circuit indicates that it will use less than 10% of the available peripheral area on the existing CMOS backplane. This demonstrates that the CE-RRC has a high potential for integration onto a future design with little or no impact on the die area and cost.

In summary, this CE-RRC achieves two significant goals. They are as follows:

(1) data conversion from 3-to-4 coordinates using minimum system resource,

(2) application of the WSP% to compensate the generic colour issue inherent in the RGBW system.

4 Software simulation

The purpose of the evaluation of simulated images is to check for visible contour artefacts and noticeable colour variations between a representative selection of pairs of image where each pair comprises a virtual RGB image and the corresponding virtual RGBW image. The RGB data of sample images are decoded and encoded with a gamma of 2.2 before and after processed by CE-RCC (Fig. 9). After that, these simulated images are inspected visually by displaying them on a high resolution monitor. In addition, the viewing distance of the simulated image is adjusted according to the spatial resolution of the virtual pixel.

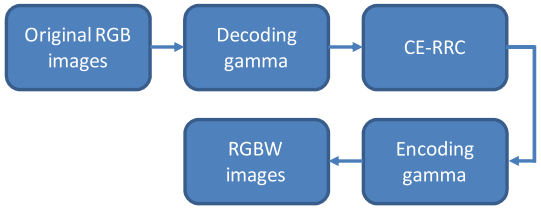

FIGURE 9 — Data processing of simulated RGBW images.

A simulated image is composed of a virtual RGBW pixel that is formed by two real RGB pixels on the display screen. One of the real pixels represents the RGB sub-pixel that shows values R″, G″ and B″, whereas the other real pixel is a virtual WSP to represent the value of W″ (WR, WG and WB). The virtual RGBW pixel configuration is illustrated as Fig. 10.

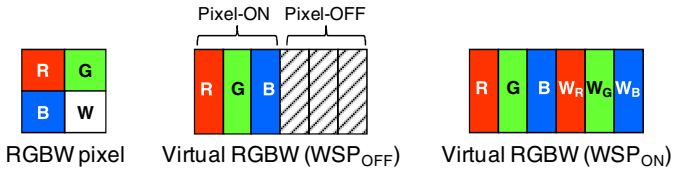

FIGURE 10 — A virtual RGBW pixel composed of two RGB pixels.

To allow for the 25% area reduction of each sub-pixel in the RGBW pixel configuration, the virtual pixel is further modified to be formed by eight RGB pixels. In each set of four virtual pixels on the screen, one is always off in order to simulate the area loss (Fig. 11).

To study the actual hardware implementation of the RGBW OLED microdisplay, the image evaluation is based on the differences between the RGB mode (virtual RGBW pixel with WSP-OFF) and the RGBW mode (virtual RGBW pixel with WSP-ON). This comparison of two driving modes gives some indication of the change in image quality after white replacement by the WSP. The summary of the arrangement of RGB pixels in different configurations of the virtual pixel is listed in Table 1.

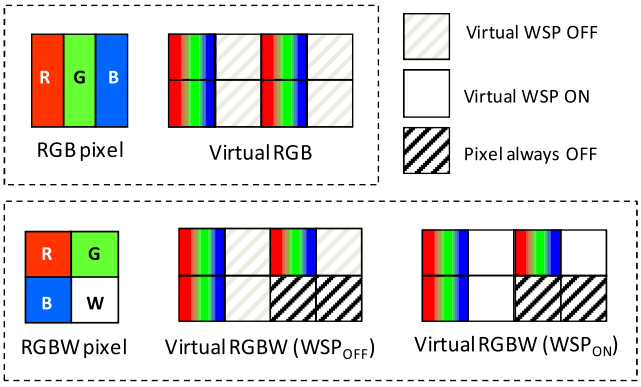

FIGURE 11 — Virtual RGBW pixels with area loss compensation

To account for the reduction of spatial frequency in the virtual RGBW image for the visual evaluation, the viewing distance of the simulated images is increased to avoid the perception of individually distinguishable pixels. The viewing distance (D) measured in centimetre is calculated using Eq. (4),[30] where is the angle of the human visual acuity, PD is the

pixel density of the sample picture, N_H is the number of horizontal pixels in the picture and L_W is the width of the picture (Fig. 12).

$$PD = \frac{N_H}{L_W}, \theta = \frac{1}{60^\circ}$$
$$D = \frac{PD}{2\tan\left(\frac{\theta}{2}\right)} = \frac{3438}{PD} \quad (4)$$

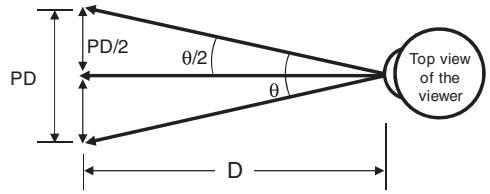

FIGURE 12 — Viewing distance definition.

4.1 Results

Examples of the simulated images that are displayed on an LCD monitor, after gamma correction, were captured by a digital camera and displayed in Fig. 13. These images are intended only for *relative* comparison between each pair of simulated images in the visual experiments, and it must be noted that, although some characteristics of these printed images are different from the images viewed on the screen, nevertheless, we have compared both the screen images and the printed images so our conclusions remain valid.

Each sample picture has a specific purpose in the evaluation. The purpose for each image is as follows:

(1) "Balloon" shows how the CE-RRC handles highly saturated colour content.
(2) "Face" shows how the CE-RRC handles natural colours and fine details in the image.
(3) "Vegetable" shows how the CE-RRC handles a natural image with gradient changes in colours.
(4) "Text content" shows how the CE-RRC handles high white content in the image.

The simulated RGBW images show no noticeable contouring and show no significant colour variations compared with those of the RGB pixel configuration. Therefore, this image evaluation of the CE-RRC in the software design flow gives a successful result, and the software model is next transformed into hardware programme code for the hardware implementation.

4.2 Assumption of power saving

As a comparison of power saving between WSP-ON (RGBW mode) and WSP-OFF (RGB mode), the "OLED microdisplay with RGBW pixel configuration" can be interpreted as different data signals (drive levels) being applied to each sub-pixel. The effect of power saving by turning on WSPs in the RGBW OLED microdisplay is listed in Table 2. The calculations of power saving in

TABLE 1 — The arrangement of RGB pixels in different virtual pixel configurations.

Image evaluation stage	Comparison	
	Real image	Simulated image
Software Floating-point calculation	R G B vs R G B W RGB pixel vs RGBW pixel	Virtual Full RGB vs Virtual RGBW (WSP_{ON})
Software Fixed-point calculation	R G B vs R G B W RGB pixel vs RGBW pixel	Virtual Full RGB vs Virtual RGBW (WSP_{ON})
Hardware Fixed-point calculation	R G B W vs R G B W RGBW (W_{OFF}) vs RGBW (W_{ON})	Virtual RGBW (WSP_{OFF}) vs Virtual RGBW (WSP_{ON})

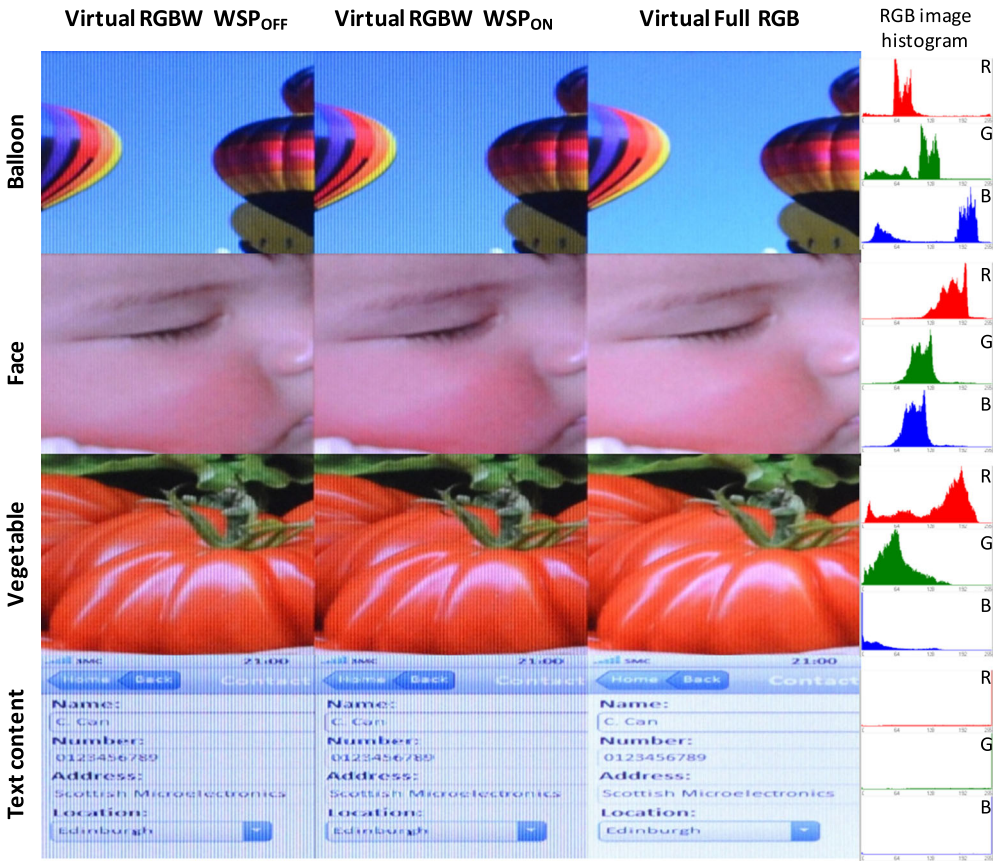

Virtual RGB WSP_{OFF}	Virtual RGB WSP_{ON}	Virtual Full RGB	Visual difference
Less bright than FULL RGB but same as WSP_{ON}	Less bright than FULL RGB but same as WSP_{OFF}	Brighter than WSP_{OFF} & WSP_{ON}	**Brightness**
Less colourful than FULL RGB but same as WSP_{ON}	Less colourful than FULL RGB but same as WSP_{OFF}	More colourful than WSP_{OFF} & WSP_{ON}	**Colourfulness**
Less sharp than FULL RGB but same as WSP_{ON}	Less sharp than FULL RGB but same as WSP_{OFF}	Sharper than WSP_{OFF} & WSP_{ON}	**Image sharpness**

FIGURE 13 — Examples simulated images captured by a digital camera.

TABLE 2 — Drive levels statistics of different pixel configurations.

After WSPs are turn on	Balloon	Face	Vegetable	Text content
Power saving (%)	30.53	42.91	21.93	60.96
Overall drive level reduction of red sub-pixel (%)	60.94	48.47	18.47	93.11
Overall drive level reduction of green sub-pixel (%)	49.60	72.56	41.14	91.54
Overall drive level reduction of blue sub-pixel (%)	34.56	81.97	78.26	89.72

percentage and overall drive level reduction of each colour sub-pixel are obtained by follow equations:

$$\text{Power saving} = \frac{\text{Total}_{\text{RGB}} - \text{Total}_{\text{RGBW}}}{\text{Total}_{\text{RGB}}} \times 100\%$$

$$\text{Overall drive level reduction of each colour channel} = \frac{\text{Total}_{C'} - \text{Total}_{C''}}{\text{Total}_{C''}} \times 100\%$$

where $\text{Total}_{\text{RGB}}$ is total value of the drive levels in RGB mode, $\text{Total}_{\text{RGBW}}$ is total value of the drive levels in RGBW mode, $\text{Total}_{C'}$ is total value of the drive levels in one of the RGB inputs and $\text{Total}_{C''}$ is total value of the drive levels in one of the RGB outputs.

The overall drive level reduction of each colour channel is not same as the power saving of the RGBW OLED microdisplay. It characterizes how the CE-RRC reacts on different white contents of the graphic input. In additions, the results in Table 2 show that there are high level of drive level reductions after using WSPs. This brings down the drive

signal of the colour pixels and avoids them to drive at high operating conditon in order to improve the usage lifetime of the OLED device.[31]

5 Real-time optional measurement

For the purposes of optical characterization, the emission of the OLED microdisplay is assumed to be Lambertian. The emission pattern of the WOLED, although not ideally so, is close to Lambertian.[32] In particular, the RGBW OLED microdisplay has a WOLED emitter with sub-pixels covered by RGB CFs to generate the primary colours. A microdisplay with a small pixel pitch may exhibit local optical crosstalk originating from adjacent colour sub-pixels,[33] and the microcavity structure inherent in the complex stack of layer in the top emission WOLED.[34,35]

However, the aim of the optical measurement is to determine the difference between the RGB mode and the RGBW mode of the microdisplay with the same system configurations. Any error that arises from assuming that the microdisplay is a Lambertian emitter in this optical measurement is comparatively unimportant because this error is common to both and it is largely cancelled in the comparison. So, to simplify calculations, the microdisplay is assumed to be a Lambertian emitter. Therefore, the radiance emitted from the microdisplay is independent of the angle of emission.

A calibrated Minolta Chroma metre CS-100 is used to measure the colour and luminance of the RGBW OLED microdisplay under two different driving modes—WSP-ON and WSP-OFF. Any difference between the measured results for the two modes is used to estimate the performance of the CE-RRC in terms of power saving and minimal colour shift. The measurement setup is illustrated in Fig. 14.

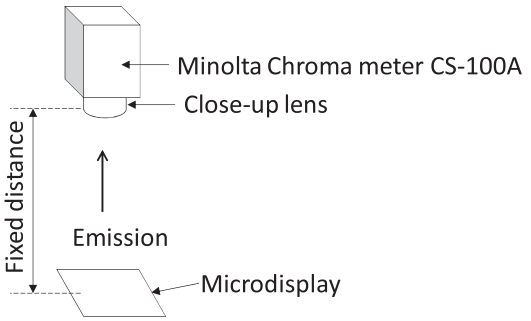

FIGURE 14 — Schematic view of the colour and luminance measurement setup.

To evaluate the performance of the CE-RRC, sample colours from the "Macbeth color checker"[36] are used as references. The results of greyscale sample in the Macbeth color checker are listed in Table 3.

In Table 3, the WSP% is 95%. All grey colours are displayed on the RGBW OLED microdisplay when the WSPs are switched ON. The maximum colour deviation is less than the TCO 06 standard[37] required to display a colour in "different areas on the same display."

In addition, if switching between RGB mode and RGBW mode on the microdisplay is considered to be, in effect, switching between two different displays, the colour tolerance defined by the Video Electronics Standards Association[38] can be up to u′ v′ equal to 0.04. In this case, the setting of WSP% at 95% can give optimal luminance output (extra luminance) to the OLED microdisplay but also maintain a reasonable colour performance in relation to the standard.

For non-neutral colours, a different value of WSP% is applied. The range varies from 90% to 65% based on each RGB input corresponding to different CIL combinations (Fig. 8). A lower CIL combination is applied to smaller values of WSP% to eliminate the effect of Weber's law.[39] The u′v′ of some colour samples (colour description in the "Macbeth color checker" from "light skin" to "orange yellow") are plotted on the CIE u′v′ diagram individually (Fig. 15) to visualize the colour shift in the colour tolerance circle.

In Fig. 15, the denotations are:

CT 0.04: colour tolerance $\Delta u'v' = 0.04$	Colour_RGB: colour composed by RGB sub-pixels only
CT 0.01: colour tolerance $\Delta u'v' = 0.01$	Colour_RGBW: Colour composed by RGBW sub-pixels

The performance of the CE-RRC is thus quantified by the optical measurements. The luminance and chromatic information of the RGBW OLED microdisplay switching between the RGB mode and RGBW mode are measured. The results reported in Fig. 15 show that most of the colour information can be kept below the maximum standard colour tolerance by CE-RRC after the white content of the RGB inputs is replaced by the WSP.

TABLE 3 — Results of Macbeth grey colour samples.

	RGB inputs			RGBW outputs				TCO 06 $\Delta u'v'$ (<0.010)	Extra luminance cd/m^2
	R′	G′	B′	R″	G″	B″	W″		
White 9.5	245	245	243	15	15	13	230	0.007	27%
Neutral	200	202	202	10	12	12	190	0.009	27%
Neutral	161	163	163	9	11	11	152	0.009	25%
Neutral	121	121	122	7	7	8	114	0.009	22%
Neutral	82	84	86	5	7	9	77	0.009	10%
Black 2	49	49	51	3	3	5	46	0.010	7%

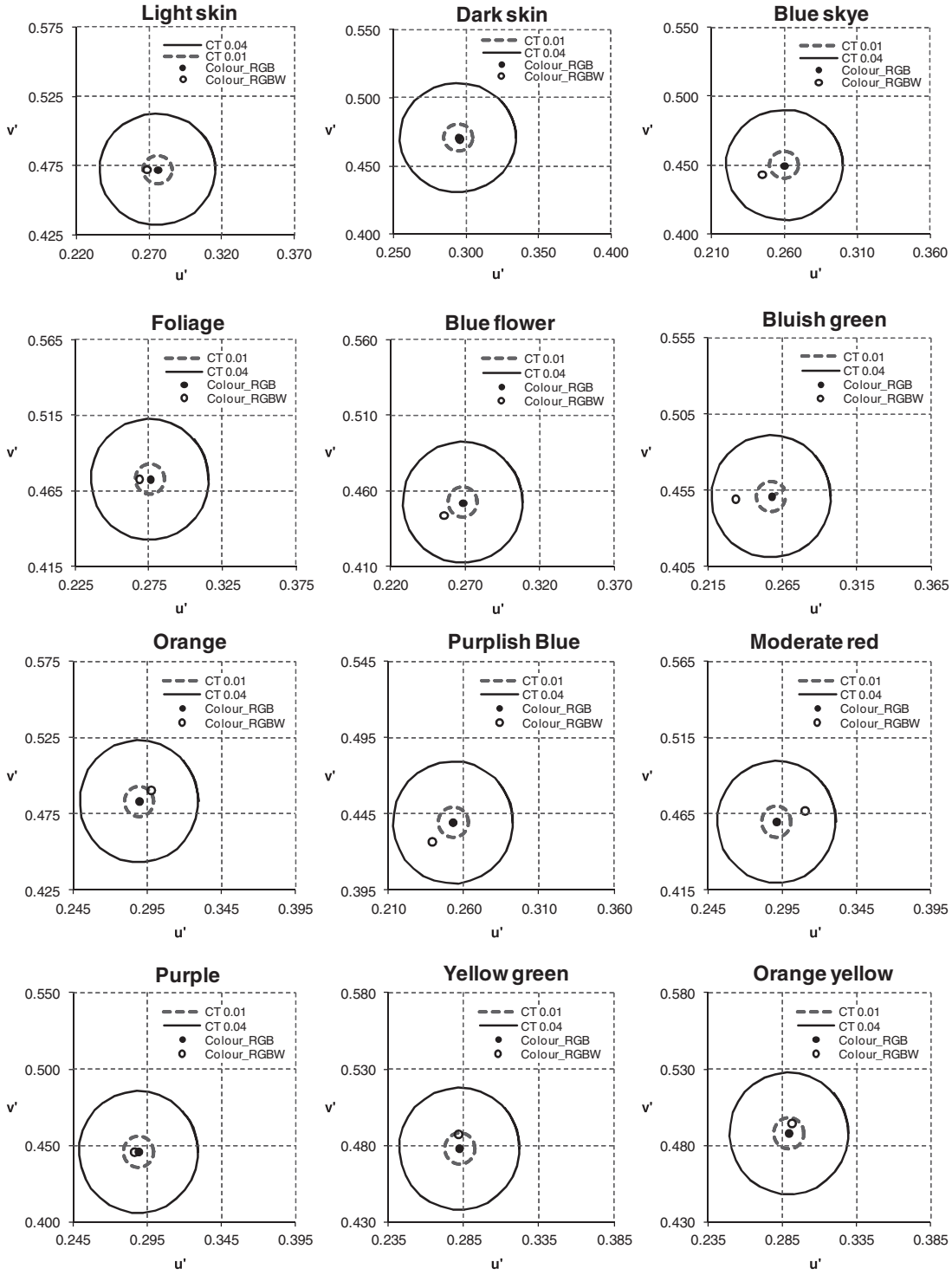

FIGURE 15 — CIE u′v′ map of Macbeth colour samples.

6 Conclusion

In conclusion, the primary benefit of the quad-pixel RGBW design is to decrease the power consumption of the OLED microdisplay for a given image luminance. The proposed method of RGB-to-RGBW data conversion, namely the CE-RRC, offers a very low overhead 3-to-4 point data conversion that achieves not only the efficient data conversion but also maintains the potential of the RGBW OLED microdisplay to fully realize the concept of DSoC. Finally, the results of the co-design flow of the algorithm development show the potential for the CE-RRC to achieve an acceptable image quality and to be integrated into the microdisplay backplane with no significant effect on the die size.

Acknowledgments

The authors thank the MicroOLED for the supply of microdisplays. Especially the technical support from Dr Gunther Haas and Denis Sarrasin in this project is very important. We also gratefully acknowledge the assistance of Dr Chris Yates in setting up the system and protocol used for the optical measurements.

References

1 A. Arkhipov *et al.*, "Adaptive white extension for peak luminance increase in RGBW AMOLED," *SID Symp. Digest of Tech. Pap., SID* **40**, No. 1, 931–934 (2009).
2 Y. Xiong *et al.*, "Performance analysis of PLED based flat panel display with RGBW sub-pixel layout," *Org. Electron.* **10**, No 5, 857–862 (2009).
3 R. S. Cok and J. D. Shore, "White-emitting OLED devices in an RGBW format with microelement white subpixels," *J. Soc. Inf. Disp., SID*, No 9, 621–628 (2010).
4 B. W. Lee *et al.*, "Late-news paper: TFT-LCD with RGBW color system," *SID Symp. Digest of Tech. Pap., SID*, **34**, No 1, 1212–1215 (2003).
5 A. Arkhipov *et al.*, "Increasing peak luminance using white extension in RGBW AMOLED," *Proc. 27th Int. Disp. Res. Conf.* **1**, 204–206 (2007).
6 O. Prache, "Full-colour SVGA + OLED-on-silicon microdisplay," *J. Soc. Inf. Disp., SID*, **10**, No 2, 133–138 (2002).
7 M. Kimura *et al.*, "Low-temperature polysilicon thin-film transistor driving with integrated driver for high-resolution light emitting polymer display," *Electron Devices, IEEE Trans.* **46**, No 12, 2282–2288 (1999).
8 G. Levy et al., "An 852 x 600 pixel OLED-on-silicon color microdisplay using CMOS subthreshold-voltage-scaling current drivers Solid-State Circuits," *IEEE J.*, **37**, No 12, 1879–1889 (2002).
9 G. Kelly *et al.*, "A full-color QVGA microdisplay using light-emitting-polymer on CMOS electronics, circuits and systems," *ICECS '06. 13th IEEE Int. Conf. on 2006*. **2**, 760–763 (2006).
10 A. Carroll and G. Heiser, "An analysis of power consumption in a smartphone," *Proc. 2010 USENIX conf., USENIX Assoc.* 21–21 (2010). http://www.nicta.com.au/pub?id=3587
11 W. Howard and O. Prache, "Microdisplays based upon organic light-emitting diodes," *IBM J. Res. Dev. IBM Corp.* **45**, No 1, 115–127 (2001).
12 I. Underwood *et al.*, "Polymer OLED microdisplay technology: pixel design in context," *Org. Light Emitting Mater. and Devices X, SPIE*, **6333**, No. 1, 633306: 1–10 (2006).
13 F. Ventsch *et al.*, "Towards organic light-emitting diode microdisplays with sub-pixel patterning," *Org. Electron.* **11**, No. 1, 57–61 (2010).
14 P. Burrows *et al.*, "Achieving full-colour organic light-emitting devices for lightweight, flat-panel displays," *Electron Devices, IEEE Trans.* **44**, No. 8, 1188–1203 (1997).
15 T. Hatwar *et al.*, "High-efficiency white OLEDs based on small molecules," *Soc. Photo-Optical Instrum. Eng. (SPIE) Conf. Ser.* **5214**, 233–240 (2004).
16 D. Y. Kondakov *et al.*, "Invited paper: OLED aging mechanisms: from fluorescence quenchers to nonradiative recombination centers," *SID Symp. Digest of Tech. Pap., SID* **34**, No. 1, 1068–1071 (2003).
17 R. S. Cok and F. Leon, "Active compensation for OLED aging," *SID Symp. Digest of Tech. Pap., SID*, **37**, No. ,1, 905–908 (2006).
18 P. Landman *et al.*, "An integrated CAD environment for low-power design," *Des. Test of Comput., IEEE* **13**, No. 2, 72–82 (1995).
19 K. Jack, "Video demystified: a handbook for the digital engineer," 5th (ed.). Newnes: Burlington, USA, 6–14 (2007).
20 H. Tanioka, "US Patent 5929843 - Image processing apparatus which extracts white component data," (1999).
21 S. D. Lee *et al.*, "US Patent 20030151694 - Method and apparatus for changing brightness of image," (2003).
22 S. Hirano *et al.*, "US Patent 7277075 - Liquid crystal display apparatus," (2007).
23 J. W. Hamer *et al.*, "US Patent 2008/0252797 A1 - Method for input-signal transformation for RGBW displays with variable W color," (2008).
24 T. Ito, "US Patent 4989080 - Color correction device with a hue area judgment unit to determine correction parameters," (1991).
25 S. D. Lee and C. Y. Kim, "US 5867286 - Color processing method and apparatus thereof using two-dimensional chromaticity separation," (1999).
26 A. Kunzman, "US Patent 6256425 - Adaptive white light enhancement for displays," (2001).
27 M. J. Murdoch *et al.*, "US 2004/0263528 A1 - Method for transforming three color input signals to four or more output signals for a color display," (2004).
28 Y. I. Han *et al.*, "US Patent 2004/0036704 - Adaptive contrast and brightness enhancement with color preservation," (2004).
29 J. Rabaey *et al.*, "Low power design methodologies," Kluwer academic publishers: Norwell, MA **118**, 289–334 (1996).
30 H. O. Knoche and M. A. Sasse, "The sweet spot: how people trade off size and definition on mobile devices," *Proc. 16th ACM Int. Conf. on Multimedia ACM*, 21–30 (2008).
31 A. R. Buckley *et al.*, "Towards a generic OLED lifetime model," *J. Soc. for Inf. Disp., SID* **17**, No. 7, 611–616 (2009).
32 G. He *et al.*, "White stacked OLED with 38 lm/W and 100,000-hour lifetime at 1000 cd/m^2 for display and lighting applications," *J. Soc. for Inf. Disp., SID* **17**, No. 2, 159–165 (2009).
33 A. R. Buckley and C. Yates, "Colour Optoelectronic Device," US Patent 2010/0283068 A1, (2010).
34 I. Underwood *et al.*, "P-OLED Microdisplay Technology," IMID/IDMC 2006 Digest, 6–1, 105–110 (2006).
35 M. Thomschke et al., "Optimized efficiency and angular emission characteristics of white top-emitting organic electroluminescent diodes," AIP. **94**, No. 8, 083303 (2009).
36 The BabelColor Company, "ColorChecker," http://www.babelcolor.com/main_ level/ColorChecker.htm (Accessed on 10th,September, (2012)
37 TCO, "TCO'06 media displays 1.2," TCO Development, (2006), 74–83.
38 VESA, "Flat panel display measurement (FPDM) standard version 2.0", Video Electronics Standards Association (VESA) Display Metrology Committee, 115–124 (2001).
39 G. Wyszecki and W. Stiles, "Color Science: Concepts and Methods, Quantitative Data and Formulas," 2nd edition, Wiley: New Jersey (United States), 490–499 (2000).

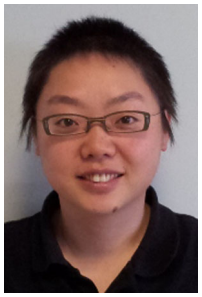

Chi Can received her MS degree in Colour Physics from the University of Leeds in 2002 and her PhD in electronics engineering from the University of Edinburgh in 2012. Before her PhD study, she worked in Taiwan as an R&D engineer in the LCD industries. Her PhD research was on colour optimization applied to the display-system-on-chip. Related areas of expertise include colour engineering and image quality evaluation.

Ian Underwood is the Head of the Institute for Integrated Micro and Nano Systems (IMNS) and Professor of Electronic Displays at The University of Edinburgh. Previously, he was a co-founder of Micro-Emissive Displays (MED) and co-inventor of its P-OLED microdisplay technology. Major honours include the Ernst & Young Emerging Entrepreneur of the Year, Scotland (2003), Fellow of the Royal Society of Edinburgh (2004), Gannochy Medal for Innovation winner (2004), Fellow of the Royal Academy of Engineering (2008) and Fellow of the Institute of Physics (2008). He is the co-author of the book entitled Introduction to Microdisplays (Wiley, 2006) and is recognized worldwide as an authority on microdisplay technology, systems and applications. Until recently, he sat on the Scottish Science Advisory Council.